On-surface Synthesis of One-dimensional Carbon-based Nanostructures via C-X and C-H Activation Reactions

Faming Kang and Wei Xu*[a]

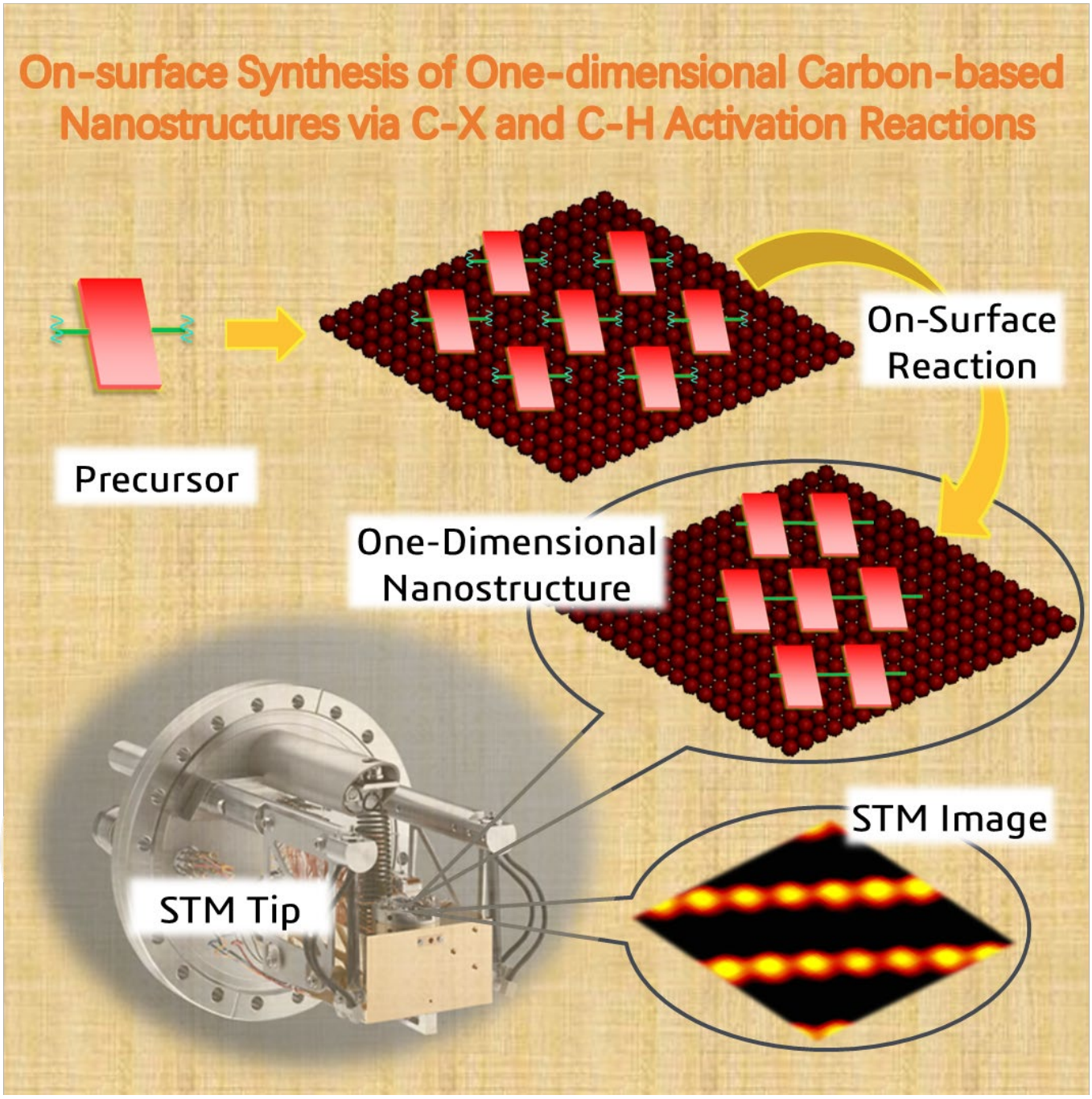

Abstract: The past decades have witnessed the emergence of low-dimensional carbon-based nanostructures owing to their unique properties and various subsequent applications. It is of fundamental importance to explore the way to achieve atomically precise fabrication of these interesting structures. The newly developed on-surface synthesis method provides an efficient strategy for this challenging issue, which demonstrates the potential of atomically precise preparation of low-dimensional nanostructures. Up to now, the formation of various surface nanostructures, especially carbon-based ones, such as graphene nanoribbons (GNRs), kinds of organic (organometallic) chains and films, have been achieved via on-surface synthesis strategy, in which in-depth understanding of the reaction mechanism has also been explored. This review article will provide a general overview on the formation of one-dimensional carbon-based nanostructures via on-surface synthesis method. In this review, only a part of the on-surface chemical reactions (specifically, C–X (X = Cl, Br, I) and C–H activation reactions) under ultra-high vacuum (UHV) conditions will be covered.

1. Introduction

Low-dimensional carbon-based materials have always attracted considerable interests for their extraordinary electronic and optical properties[1]. For example, Shirakawa[2] and coworkers successfully synthesized iodine-doped *trans*-polyacetylene after the exposure of *trans*-polyacetylene to iodine vapor, which was found to have a remarkably high conductivity at room temperature (RT). For centuries, chemists performed reactions mainly in solution phase or solid-liquid interfaces (surfaces usually act as catalysts), with the aim to prepare these potential low-dimensional carbon nanomaterials. A series of important achievements have been reported within the field of carbon allotropes[3]. While, it is relatively hard to make atomically precise single-layer nanostructures in solution chemistry. On the other hand, with the increasing size of the nanostructures, the reduction of stability appears, which leads to intermolecular polymerization and cross-linked systems[4].

On-surface synthesis under the UHV condition is a newly emerged strategy for the preparation of low-dimensional nanostructures[5,6]. In comparison with the traditional solution-based chemistry, on-surface chemical reactions carried out under the UHV environments could eliminate possible influence from surroundings, which benefits for the preparation of atomically precise nanostructures. Furthermore, metal surfaces could be employed as both catalysts and templates so that some reactions can be facilitated due to the surface confinement effect.

[a] F. Kang, Prof. Dr. W. Xu
Interdisciplinary Materials Research Center and College of Materials Science and Engineering, Tongji University
Shanghai 201804, P. R. China
E-mail: xuwei@tongji.edu.cn

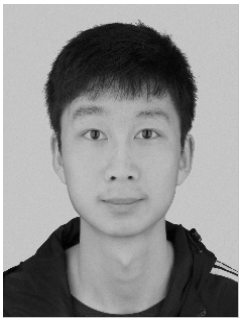

Faming Kang was born in 1994 and studied Materials Science at Tongji University. Since 2018 he has investigated the chemical reactions on single-crystal surfaces under ultra-high vacuum conditions by scanning tunnelling microscope for his master program in the group of Prof. Wei Xu.

Prof. Wei Xu received his PhD degree in Science from Aarhus University, Denmark in 2008. Whereafter he was a postdoctoral fellow at Interdisciplinary Nanoscience Center (iNANO), Aarhus University, Denmark and at Departments of Chemistry and Physics, The Penn State University, USA. Since 2009 he has been a full professor at Tongji University, P. R. China. His main research interests are Scanning Tunneling Microscopy (STM) and Density Functional Theory (DFT) investigations of molecular self-assemblies and reactions on surfaces under ultra-high vacuum conditions with the aim of controllably building functional surface nanostructures and gaining fundamental insights into physics and chemistry.

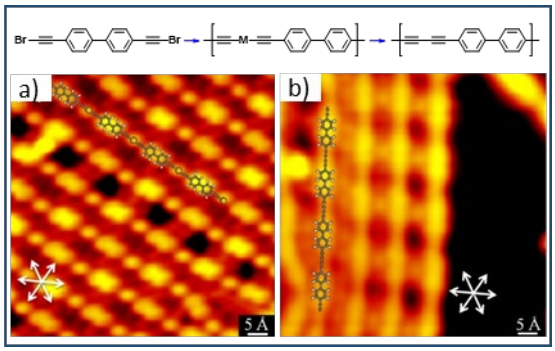

Figure 1. (a) STM image showing the formation of the C−Au−C organometallic chains on Au(111). The scaled model of a C−Au−C chain is overlaid on the corresponding STM topography. (b) STM image showing the formation of the C−C coupled molecular chains with acetylenic scaffoldings after the sample is annealed to ~ 425 K. (Adapted with permission from ref. [8]. Copyright 2016 by the American Chemical Society.)

The invention of scanning tunneling microscope (STM) by Binnig and Rohrer in 1981[7] makes it possible for us to analyze the atomic structures adsorbed on the surface. Meanwhile, STM tip could also be employed to in-situ locally induce surface reactions. Accordingly, STM is an appropriate tool to explore on-surface chemical reactions for now. As a surface-sensitive quantitative spectroscopic technique, X-ray photoelectron spectroscopy (XPS) enables the measurement of elemental composition of structures and chemical state of the elements, which could provide supplementary information for analyzing surface supported nanostructures. Moreover, density functional theory (DFT) calculations are widely employed to understand the reaction mechanism.

Since carbon is one of the most basic elements in nature, it is of great significance to study the carbon-based nanostructures/ nanomaterials. The following content of this review will mainly focus on the preparation of one-dimensional structures via various dehalogenative and dehydrogenative homocouplings of sp-, sp^2- and sp^3-carbon on surfaces.

2. C–X and C–H activation of sp-carbon

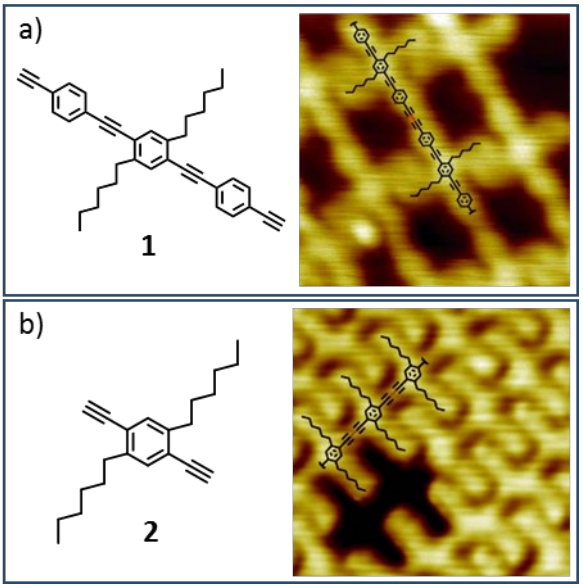

Figure 2. (a) STM image of alkyne **1** on Ag(111) after on-surface oligomerization. (b) STM image of **2** on Ag(111) after annealing . (Adapted with permission from ref. [12]. Copyright 2013 by Wiley-VCH.)

On-surface dehalogenative/dehydrogenative homocoupling reactions of precursors functionalized with alkynyl groups have manifested great potential for the fabrication of low-dimensional carbon-based nanostructures involving acetylenic scaffolds, such as carbyne, graphyne and graphdiyne. Sun[8] et al. reported the successful formation of one-dimensional wires with acetylenic scaffolding via on-surface C–Br activation of sp-hybridized carbon atoms. They designed and synthesized the precursor 4,4'-di(bromoethynyl)-1,1'-biphenyl (bBEBP), and then deposited it on Au(111) substrate at RT. After annealing to ~320 K, one-dimensional chains were formed on the surface. These chains were composed of two kinds of alternating protrusions. Thus, an organometallic chain structure combined with C–Au–C was proposed (as shown in **Figure 1a**), with the DFT model being in good agreement with the STM image. Further annealing to ~425 K leaded to Au atoms released from the organometallic chains, and consequently, C–C coupled molecular chains with acetylenic linkages were obtained (as shown in **Figure 1b**). The disappearance of dot protrusions between biphenyl groups can be observed from the STM images. Additionally, the feasibility to

incorporate acetylenic scaffoldings into two-dimensional networks was also be demonstrated in this work. Liu et al. analogously synthesized graphdiyne zigzag chains and macrocycles. Statistical results showed that macrocycles were preferred to form in low coverage of organometallic intermediates[9]. These works act as a supplement to our understandings of on-surface dehalogenative homocoupling reactions, and moreover, make C–X activation of sp-hybridized carbon a suitable strategy to synthesize high-quality nanostructures with acetylenic linkages.

Glaser coupling, discovered by Glaser[10] in 1869, can also be applied to the preparation of chain structures with acetylenic linkages. Zhang et al. first reported Glaser coupling of terminal alkynes on metal surfaces[11]. Gao[12] et al. then produced one-dimensional chains via this method. They chose 4,4'-((2,5-dihexyl-1,4-phenylene)bis(ethyne-2,1-diyl))bis(ethynylbenzene) (compound **1**) as precursor for their initial investigation. Compound **1** formed a monolayer when deposited on a Au(111) surface at RT. After annealing the **1**-covered Au(111) surface to ~398 K, the oligomer of **1** was obtained, which indicated the occurrence of the covalent coupling between the intermolecular alkyne functionalities. In order to investigate optimization method towards highly selective Glaser coupling, depositions of compound **1** on other substrates such as Au(100), Cu(111) and Ag(111) was performed as well in this work. Compared with other substrates, Ag(111) was demonstrated to be an ideal one with the highest selectivity towards Glaser coupling. As shown in **Figure 2a**, oligomeric structures appeared after annealing the compound **1**-covered Ag(111) substrate. Importantly, the abundance of the two-unit linear coupling on Ag(111) surface reached an abundance of up to (64.3±8.1) %, much higher than that obtained on Au(111) surface. Furthermore, alkyne **2** (1,4-diethynyl-2,5-dihexylbenzene) was prepared for further investigation to improve the selectivity towards Glaser coupling. Analogously, after **2** underwent the same procedure as **1**, the targeted linear chains were obtained both on Au(111) and Ag(111) substrates (as shown in **Figure 2b**). Surprisingly, the proportion of targeted linear chains on both surfaces increased to ~95 % on Ag(111). It proved that the simple steric hindrance of the alkyne could lead to the suppression of side reactions. Their work reveals the fact that the selectivity of on-surface Glaser coupling is affected by both metal substrates and precursors.

Years later, Liu[13] et al. systematically described the Glaser coupling on Ag(111), Ag(110), and Ag(100) substrates, with the obtainment of an organometallic product as well as Glaser

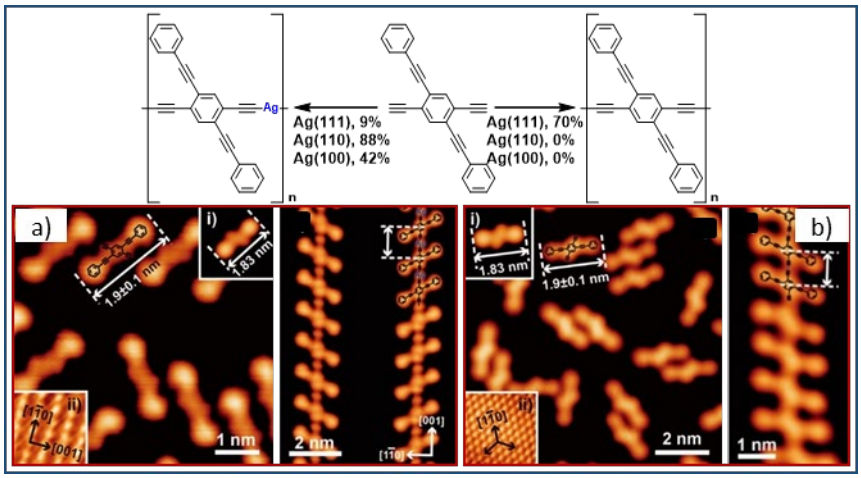

Figure 3. (a) STM images of the DEBPB molecules on Ag(110). The molecules are deposited onto the substrate, which is held at about 100 K. The chemical structure of DEBPB is superimposed. High-resolution STM image of two organometallic chains achieved by annealing at about 350 K. (b) STM images of the DEBPB molecules on Ag(111). High-resolution STM image of a Glaser-coupled covalent chain achieved by annealing at 350 K. (Adapted with permission from ref. [13]. Copyright 2015 by the American Chemical Society.)

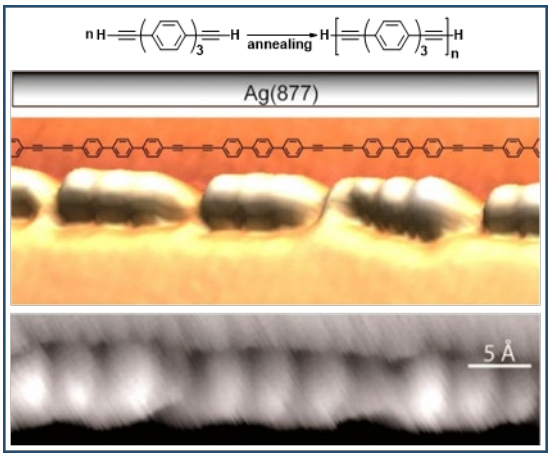

Figure 4. High-resolution STM image of a part of a terphenylene-butadiynylene wire placed at the lower step-edges. (Adapted with permission from ref. [16]. Copyright 2014 by the American Chemical Society.)

coupling product. The precursor employed was 2,5-diethynyl-1,4-bis(phenylethynyl)-benzene (DEBPB). They deposited DEBPB on Ag(111), Ag(110) and Ag(100) at about 100 K with the subsequent annealing, respectively. Thus, different major reactions took place, leading to distinct main products at similar reaction temperatures. On Ag(110) and Ag(100), the reaction between terminal alkynes and metal atoms was preferred. Hence, organometallic chains (as shown in **Figure 3a**) were produced, with the productivity (the proportion of the particular product obtained by statistical analysis) of 88 % on Ag(110) and 42 % on Ag(100). However, one-dimensional covalent molecular chains (as shown in **Figure 3b**) were formed on Ag(111) surface with a productivity of about 70 %. The above presented experimental results of this work showed that Glaser coupling of alkyne compound preferred to take place on Ag(111). The same group later reported room-temperature activation of the C–H bond in terminal alkynyl groups. It should be noticed that they observed the organometallic chains at RT and their conversion to covalent molecular chains. This anomaly may be attributed to the existence of detached Br adatoms[14]. Other competitive reactions such as cyclotrimerization were also studied. The results showed that Glaser coupling is preferred at high surface coverage[15].

Cirera[16] et al. paid close attention to the templating effect of the substrate, and reported the higher selectivity for the Glaser coupling reaction on Ag(877) than that on Ag(111) surface. They employed 4,4''-diethynyl-1,1':4',1''-terphenyl as a precursor. When molecules were evaporated onto the Ag(877) template held at 186 K for very low coverage, it can be observed by STM that molecules bind to the step edges, and their backbones are parallel to the edges. It even persisted at increased coverage. This templating effect facilitates the subsequent polymerization after annealing to 450 K. The product is a novel molecular wire belongs to the family of extended graphdiynes. High-resolution STM images (as shown in **Figure 4**) showed that the newly formed covalent linkages appeared as depressions while benzene rings appeared as bright protrusions in the groups of three. Cirera's work highlights the impact of the morphology of substrate on reaction pathways, which promotes the advancement of covalent bottom-up nanofabrication strategies.

In the last decades, carbon allotropes with acetylenic scaffolds especially graphyne-like nanostructures have attracted a lot of attentions, and many remarkable results have also been

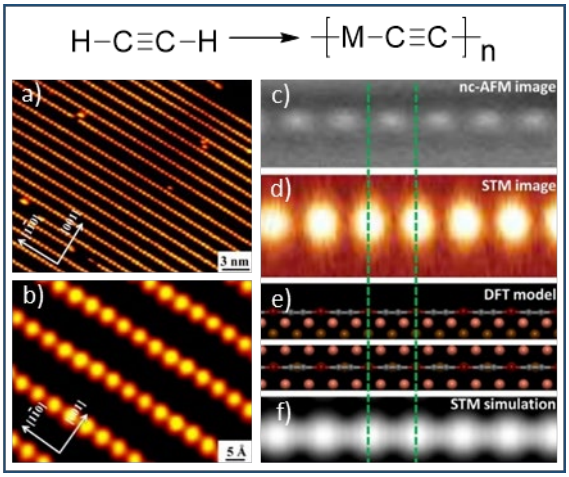

Figure 5. (a) Large-scale and (b) close-up STM images showing the formation of metalated carbyne chains. Equally scaled (c) high-resolution nc-AFM frequency shift image, (d) current image, (e) DFT-optimized model, and (f) STM simulation of a single metalated carbyne chain on Cu(110). (Adapted with permission from ref. [17]. Copyright 2016 by the American Chemical Society.)

achieved[8,16]. Inspired by these results, Sun[17] et al. focused on the bottom-up fabrication of another carbon allotrope, carbyne, and in the first step, successfully synthesized the metalated carbyne via on-surface synthesis. Ethyne molecule was chosen as a precursor, and Cu(110) was selected as the substrate. After deposition of ethyne on the surface held at ~450 K, one-dimensional chains were observed (as shown in **Figure 5**). These Chains were arranged along the close-packed [1$\bar{1}$0] direction of the substrate. According to the XPS results, two main peaks of C 1s confirmed the formation of metalated carbyne. Annealing the metalated carbyne covered sample to ~600 K, they did not achieve to release the Cu atoms from C–Cu–C structures. Additionally, images of non‑contact atomic force microscopy (nc-AFM) and DFT calculations further confirmed the proposed metalated carbyne structure. The similar experiments on Ag(110) and Au(110) surfaces indicated that the interactions between ethyne and these two surfaces are so weak that ethyne molecules would hardly stick on either of them.

3. C–X and C–H activation of sp^2-carbon

Ullmann discovered that copper powder could induce the cleavage of an aromatic C–X bond, which leads to the formation of diaryls[18]. Since that, this so-called Ullmann coupling reaction has been widely used, and became one of the important reactions in organic synthesis. The first attempt at realizing Ullmann coupling on the surface was practiced by Hla[19] and coworkers. They performed STM tip manipulation to induce the cleavage of C–I bond as well as the subsequent covalent coupling of two phenyl moieties after depositing iodobenzene (C_6H_5I) onto the Cu(111) surface. Two phenyls were finally brought together spatially, indicating the formation of biphenyl. Their success declared that free phenyl radical can be stabilized by the interaction with metal substrate comparing its short lifetime in solution. STM tip manipulation is a harsh trigger to induce a chemical reaction, and accordingly, this is not an efficient strategy for the fabrication of low-dimensional nanostructures. Years later, Grill[5] and coworkers developed a new strategy by simply annealing the molecule covered sample to induce the cleavage of C–X bond and subsequent C–C coupling, which becomes a more

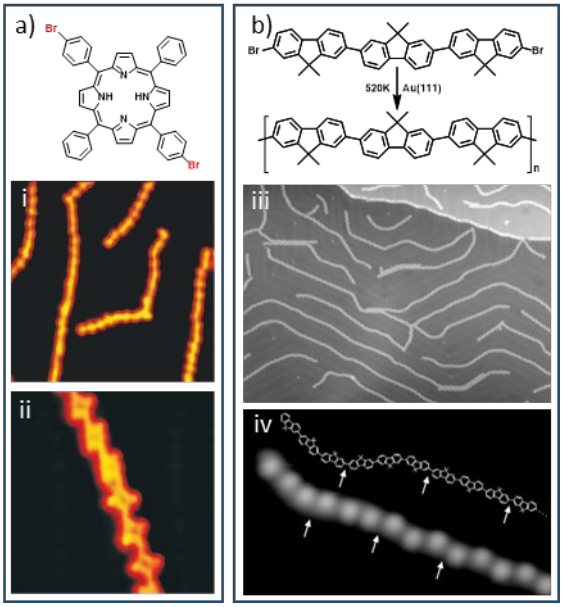

Figure 6. (a) Overview STM image (i) and the detailed one (ii) of the nanostructures formed by Ullmann coupling. (b) Overview STM image after on-surface polymerization (iii). (iv) STM image of a single polyfluorene chain end with its chemical structure superimposed (using a different scaling). The arrows indicate three identical (in the STM image and the chemical structure), newly formed covalent bonds between individual building blocks. (Adapted with permission from ref. [5] and [22]. Copyright 2007 by the Nature Publishing Group and copyright 2009 by the American Association for the Advancement of Science.)

widely used method for on-surface reactions. They designed and synthesized different TPP-based molecules (TPP equals to 5,10,15,20-tetra(phenyl)porphyrin): Br–TPP for dimer, *trans*-Br_2TPP for one-dimensional chain, and Br_4TPP for two-dimensional network. For special attention on one-dimensional nanostructures, long linear chains are formed after the deposition of *trans*-Br_2TPP on Au(111) and subsequent annealing (as shown in **Figure 6a**). It is noted that some conspicuous abrupt curvatures existed in the middle of some chains, caused by the attachment of two chains upon weak interaction. Later, Lin[20] et al. demonstrated that metal substrates could serve as directing templates as well as catalysts. After deposition of the precursor (*trans*-Br_2TPP modified by N) on the Au(111) surface that

contained Cu islands at RT, single-row organometallic chains were observed, which were caused by pyridyl-Cu-pyridyl coordination. Double or triple rows of monomers appeared after annealing at 453 K, revealing the occurrence of the Ullmann coupling. Adisoejoso[21] et al. further studied the mechanism of Pd-catalyzed and Cu-catalyzed homocoupling of aryl bromide, and *trans*-Br_2TPP was chosen as precursor again. They eventually concluded that these two different catalysts account for different mechanisms — Cu-catalyzed reaction rate is determined by C–Br activation step while Pd-catalyzed one is determined by C–C formation step.

Besides, a considerable amount of success has been achieved in the construction of one-dimensional structures via on-surface Ullmann coupling reaction with a more in-depth explanation of the mechanism and properties. For example, Ample[22] et al. used dibromoterfluorene (DBTF) monomers to produce long molecular chains. The well-defined polymer chains randomly diffused on the Au(111) surface after annealing the sample at 520 K (as shown in **Figure 6b**). Vertical manipulation was performed to measure the statistical relationship between the conductance of a single wire and the distance between the two contact points on the wire.

The results showed that the contact conductance is oscillating due to the multistage feature of the wire. The same group then presented a method to adsorb a molecular wire both on metallic and insulating (NaCl) surface areas[23]. They performed a comparative test to investigate the effect of the different deposition order of NaCl and DBTF. They discovered that only when depositing NaCl after DBTF, the chain could be adsorbed partly on the metal and partly on top of NaCl. It indicates that the interactions between the polymer chains and the gold substrate are weak. Saywell[24] et al. studied the adsorption of DBTF molecules on a stepped Au(10,7,7) surface and claimed that the surface steps could serve as catalytically active sites as well as the template in comparison with the flat Au(111) surface.

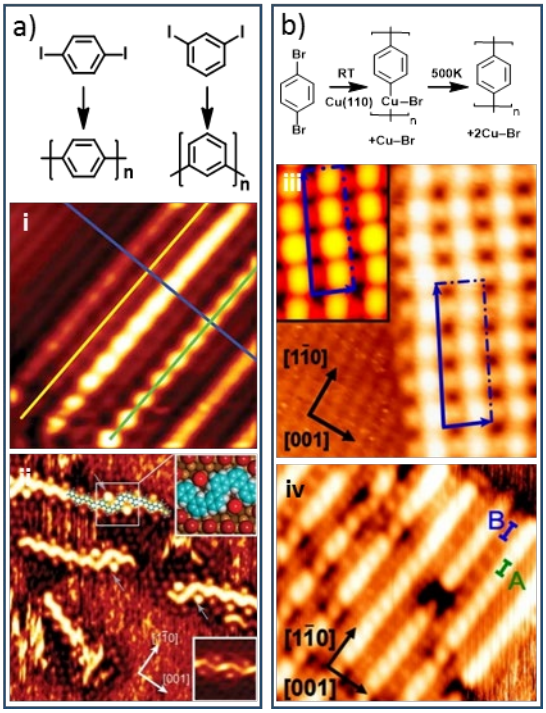

Figure 7. (a) STM images of (i) linear polymerized chains formed by 1,4-diiodobenzene molecules, and (ii) branched chains formed by 1,3-diiodobenzene on Cu(110). (b) STM images of (iii) organometallic chains and (iv) C-C coupled polymerized chains. (Adapted with permission from ref. [25] and [27]. Copyright 2009 by Wiley-VCH and copyright 2013 by the American Chemical Society.)

Soon after Grill's work, Lipton-Duffin[25] et al. reported the on-surface synthesis of linear and zigzag chains (poly(p-phenylene), PPP and poly(m-phenylene), PMP) via Ullmann coupling of 1,4-diiodobenzene and 1,3-diiodobenzene respectively (as shown in **Figure 7a** i and ii, respectively). The results showed that C–I bond cleavage also can be achieved on the surface. More importantly, some PMP chains contain kinks, whose final appearance are ring structures. It indicates that on-surface Ullmann coupling can be potentially extended to not only one-dimensional structures but also more complex structures (such as film and ring structures) with unique properties [26]. Until 2013, Di Giovannantonio[27] et al. provided the insights into dehalogenative polymerizations with the combination of STM, XPS, low energy electron diffraction (LEED), and near-edge X-ray absorption fine structure spectroscopy (NEXAFS). 1,4-dibromobenzene (dBB) was chosen as the precursor, and Cu(110) was chosen as the substrate. STM images directly displayed the formation of an organometallic structure at RT (as shown in **Figure 7b** iii) and C-C coupled polymer after annealing (as shown in **Figure 7b** iv). The results of

XPS and NEXAFS spectra indicated that the dehalogenation was complete, and copper-linked carbon existed at RT. And a combination of DFT, STM and XPS indicated that nearly half bromine atoms adsorbed on the top of the Cu atoms involved in the organometallic structure while the others positioned on the substrate.

The following works offered new insights into the mechanistic process of Ullmann coupling. Zint[28] et al. showed the complete pathway of Ullmann coupling by STM and AFM. In the same year, Zhou[29] et al. reported that the reaction pathway is influenced by whether the initially formed organometallic intermediate self-assembled or not. When intermediates are randomly dispersed, a specific clover-shaped intermediates can be identified. Di Giovannantonio[30] et al. performed kinetic analysis and concluded that the polymerization reaction is a diffusion-controlled process and follow a nucleation-and-growth behavior. Barton[31] et al. indicated that the dehalogenation process was facilitated by the adatoms.

To obtain more complicated structures, Fan[32] et al. performed the experiment by deposition of a more complicated precursor, 4,4''-dibromo-m-terphenyl (DMTP), onto the Cu(111) surface held at 300 K, mainly yielding zigzag polymer chains with C–Cu–C motifs. However, when rising the substrate temperature to 550 K, completely different structures (hexagonal rings built up of six m-terphenylene fragments) were generated. The precursor DMTP was studied by Dai[33] et al. again on Cu(110) surface (as shown in **Figure 8**). The difference between the results on Cu(111) and that on Cu(110) is that *cis*/*trans* and all-*trans* organometallic chains were formed on Cu(110) when the deposition temperature was 300 K, which is mainly attributed to the different commensurability between the organometallic chains and the substrate lattice. The deposition of DMTP onto Cu(110) held at 383 K led to the formation of all-*trans* zigzag organometallic chains, and C–C covalently bonded zigzag oligophenylene chains were obtained after annealing the organometallic chains to 458 K. The above results illustrated that substrates play an important role in the formation of one-dimensional chains. The same group later performed a similar work on Ag(111), and they found that hyperbenzene is formed in higher substrate temperatures[34].

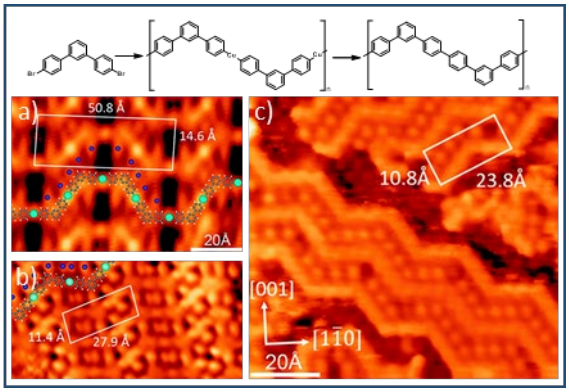

Figure 8. Intramolecular Ullmann coupling reaction of 4,4''-dibromo-m-terphenyl (DMTP) on Cu(110) surface. (a) STM image of the cis/trans chains. (b) High-resolution STM image of a section of the same all-trans zigzag structure. (c) STM image of zigzag oligophenylene chains. (Adapted with permission from ref. [33]. Copyright 2016 by the Royal Society of Chemistry.)

Liu[35] et al. obtained linear polymer chains with pentagons that were not fully coordinated by hexagons after 5,12-bis(4-bromophenyl)benzo[k]-tetraphene molecules underwent polymerization and subsequent cyclodehydrogenation on the Au(111) surface. Planarity should account for maintaining the regularity of the ribbon structure. Also, Au-directed heptacene organometallic complexes were synthesized by Urgel[36] et al. It is notable that Zhang[37] et al. showed the different contact geometries of multiple covalent aryl-Au bonds with the halogen substituents in the bay or peri regions. Specifically, gold-organic hybrid stabilized by bay-aryl-Au bonds were prepared by the deposition of tetrachloro-substituted perylene-3,4,9,10-tetracarboxylic acid bisimide (4Cl-PBI) on hot Au(111) substrate while the ones stabilized by peri-aryl-Au bonds appeared as an intermediate in the synthesis of rylene-type GNRs on Au(111) surface.

Furthermore, Sun[38] et al. successfully synthesized cumulene compound by dehalogenative homocoupling of alkenyl *gem*-dibromides (another kind of C–X activation of sp^2-hybridized carbon atoms). Due to the possibility of isomerization existing in the precursor molecule, it could be fascinating to construct one-dimensional cumulene structures.

In the field of preparing GNRs by on-surface reactions, some of the most representative achievements of Ullmann coupling have emerged. Since A.K. Geim and K.S. Novoselov[39] first obtained the graphene by mechanical exfoliation, the exploration of graphene was motivated on account of its potential technological applications. The following studies of GNRs were proposed to open a band gap for room-temperature digital logic applications. This property depending on its width, edge structures, and even atomic defects can lead to changes of the relevant performance. Thus the atomically precise synthesis of GNRs is vitally significant in further explorations. Cai[40] et al. first provided an on-surface strategy for atomically precise fabrication of armchair GNR with width N = 7. They also tried to design precursor monomers to achieve the fabrication of GNRs with more complicated shapes. For example, the chevron-type GNRs with alternating widths (N = 6 and N = 9) were successfully fabricated on the Au (111) surface. Several years later, van der Lit[41] et al. obtained nc-AFM images with a CO-terminated tip, which provides the direct evidence for the formation of the GNRs. As predicted by simulations[42], the width (N) of GNRs controls their direct gaps — the increasing of N is shown to close the gap, resulting in an array of attempts on different size GNRs. Details are available in Sun's review[43].

Since the main difference between bulk graphene and GNRs is the presence of edges in nanoribbons, the study of edge effect is underway. And naturally, GNRs with different edge types have been prepared via on-surface synthesis. Han[44] et al. reported the formation of (3,1)-chiral GNRs with characteristic corrugation. The main difference from Cai's work is that Cu(111) surface was selected as the substrate. Then de Oteyza[45] et al. specifically designed the precursor 2,2'-dibromo-9,9'-bianthryl, in which substrate-independent formation of (3,1)-chiral GNRs was achieved. Their results indicated that the precursor molecules play an important role in the formation of (3,1)-chiral GNRs on different surfaces.

Schulz[46] et al. investigated into how precursor geometry determines the growth mechanism of GNRs. They investigated the growth mechanism of GNRs by introducing the precursor 10,10'-dibromo-9,9'-bianthryl (DBBA) on Au(111), Ag(111), and Cu(111) surface, respectively, using STM and nc-AFM. They finally drew the conclusion that biradical species were more stable on Cu(111) surface owing to the stronger interaction with the surface.

Ruffieux[47] et al. showed the availability of GNRs with zigzag edge. They also confirmed that the edges could be modified by external functional groups (*e.g.*, a phenyl group), eventually transforming into fluoranthene-type subunits separated by three, four and five zigzag cusps. It is obvious that this strategy can be potentially employed to alter the GNR-substrate interaction,

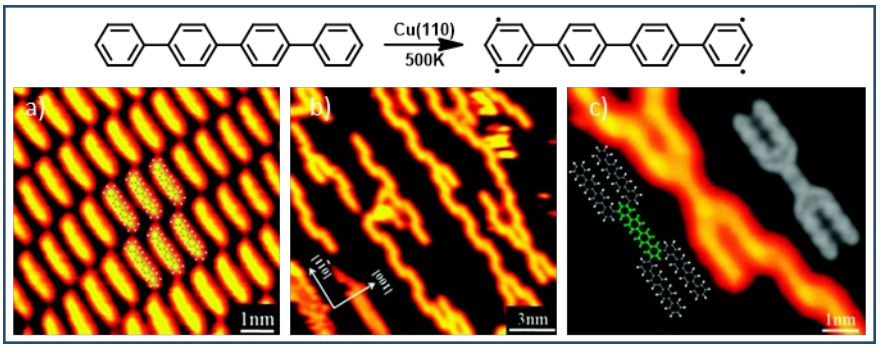

Figure 9. On-surface C–H activation of quaterphenyl (4Ph) molecules. (a) Close-up STM images of 4Ph molecules arranged on Cu(110) at a high molecular coverage. (b) STM image showing the formation of chain-like structures with branches after annealing the surface at 500 K. (c) The close-up STM image, the equally-scaled optimized structural models and the DFT-based STM image simulations (the black and white ones) of a typical structural motif within the chain structures. (Adapted with permission from ref. [49]. Copyright 2014 by the Royal Society of Chemistry.)

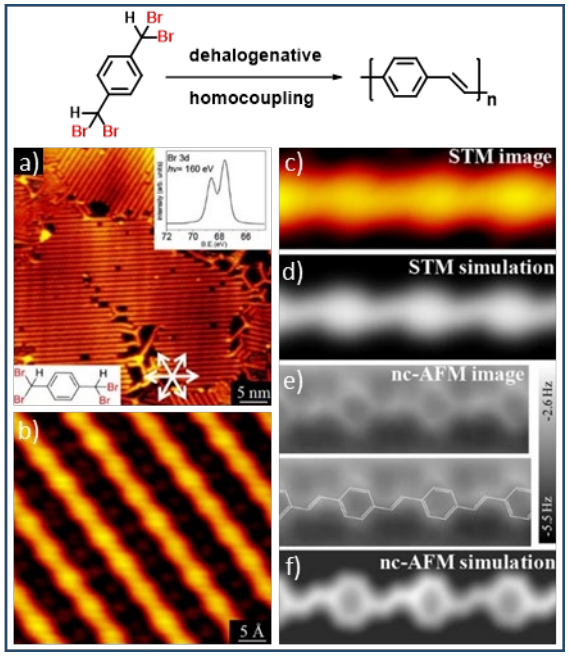

Figure 10. Formation of poly(phenylenevinylene) (PPV) by dehalogenative homocoupling reaction of 4,4'-bis(dibromomethyl)-1,1'-biphenyl (BDBMB) on Au(111) surface. (a) Large-scale and (b) close-up STM images showing the formation of PPV chains after deposition of BDBMB molecules on Au(111) held at RT and annealing to ~400 K. The XPS data of Br 3d are inserted in (a). Equally scaled (c) STM image, (d) STM simulation, (e) nc-AFM image recorded by CO-functionalized tip, with model overlaid, (f) nc-AFM simulation of a single PPV chain on Au(111). (Adapted with permission from ref. [55]. Copyright 2018 by the American Chemical Society.)

engineer the band structure of edge states, and well shield from neighboring GNRs. Besides these novel GNRs discussed above, the construction of multifunctional nanoporous graphene was successfully demonstrated[48], in which semiconducting properties of nanoporous graphene were demonstrated.

Along with C–X activation, C–H activation of sp^2-hybridized carbon atoms has also been successfully utilized in on-surface construction of one-dimensional carbon nanostructures, as reported by Sun[49] and coworkers. Limited by reaction conditions, the occurrence of selective C-H activation of aryl group was hardly achieved. Sun's work showed the feasibility of selective aryl-aryl coupling. As shown in **Figure 9**, by using the quaterphenyl (4Ph) molecule as the precursor, after deposition of the molecules on a Cu(110) surface and subsequent anneal, chain-like structures were formed, more importantly, it was found that only the meta sites of the terminal phenyl groups were activated, as demonstrated in **Figure 9c**, in which they could identify that the majority of 4Ph molecules are joined together in a uniform shoulder-to-shoulder fashion indicating the selective C–H activation and aryl-aryl coupling between 4Ph molecules. On account of the smooth and seamless electronic density of states at the molecular junctions, the covalent linkages between 4Ph molecules can be confirmed. It was also accordant with DFT-based STM image simulations.

Further improvements were performed by Cai[50] and coworkers. Direct C–H activation and C–C coupling of *para*-sexiphenyl were achieved on the Au(110) surface as well. However, for the spatial constraint at the anisotropic Au(110) surface, the four *meta*-C–H bonds lose equivalence. Besides, Wang[51] et al. reported the *para*-selective C–H activation on the Pd(111) surface, which makes on-surface C–H activation of sp^2-hybridized carbon more complete. Some other new modern studies about this theme can be ascribed to the following two works. One is that aryl azides are able to form covalent σ- and π-bonds between their transformation products on Ag(111) surface[52]. The other is that coordination interaction and self-assembly can influence the final product configurations[53].

4. C–X and C–H activation of sp^3-carbon

Wurtz reaction, another dehalogenative homocoupling reaction, was also introduced onto surfaces by Sun[54] et al. More importantly, the same group further reported the other two innovative works. Firstly, a ditopic molecular precursor (4,4'-bis(dibromomethyl)-1,1'-biphenyl, BDBMB) was introduced to fabricate a kind of intrinsic organic semiconductors, poly(phenylenevinylene) (PPV), on the Au(111) surface through successive dehalogenation and subsequent C–C homocoupling reactions[55]. After the deposition of BDBMB molecules on Au(111) held at RT, short chains were formed on the surface, and further annealing to ~400 K could improve the quality of the chain

structures. As shown in **Figure 10**, well-ordered polymer chains laid on the surface while the detached Br atoms embedded between the chains as dim protrusions. Additionally, through the nc-AFM images, the existence of C–C double bonds between the linked phenyl groups can be confirmed due to the observation of the staggered line with crossing angle ~120°.

Similarly, they provided an on-surface strategy to construct C–C triple-bonded structural motifs using tribromomethyl-substituted arenes. Poly(arylene ethynylene) (PAE) molecular chains were constructed on the Au(111) surface through dehalogenative C–C coupling[56]. 1,4-bis(tribromomethyl)benzene (bTBP) was synthesized and then deposited on Au(111) held at RT. After further annealing to 430 K, chain structures were observed (as shown in **Figure 11**) with the surrounding Br atoms. These two works demonstrated the conversion of sp^3-hybridized carbon atoms to sp^2- and sp-hybridized ones, respectively (*i.e.*, from alkyl group to alkenyl and alkynyl ones). More importantly, the halide precursors containing more than one halogen attached to the same carbon atom were employed for dehalogenative homocouplings, which enriched the on-surface synthesis strategies.

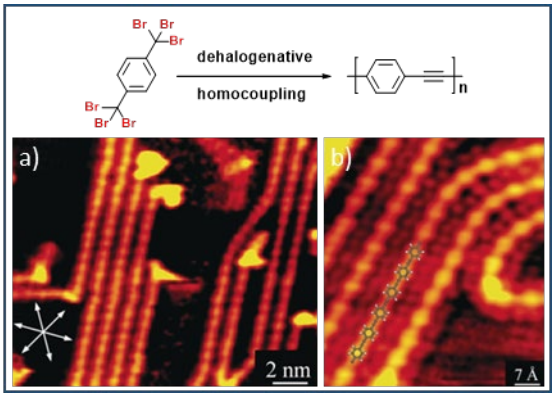

Figure 11. (a) Large-scale and (b) close-up STM images showing the formation of molecular chains (graphyne wires) after deposition of bTBP molecules on Au(111) held at room temperature followed by annealing to about 430 K. The equally scaled DFT-relaxed model is superimposed on the STM topography.(Adapted with permission from ref. [56]. Copyright 2018 by Wiley-VCH.)

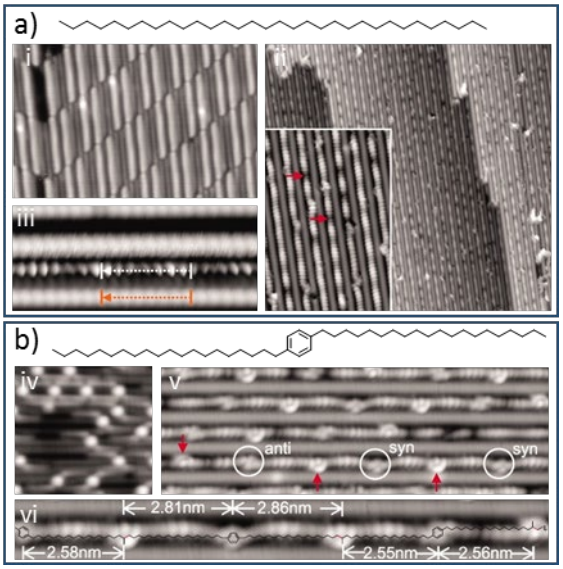

Figure 12. Intermolecular C–H activation of (a) n-dotriacontane ($C_{32}H_{66}$) and (b) 1,4-di(eicosyl)benzene (DEB) on Au(110) surface. (i) STM image of n–dotriacontane monomers deposited on Au(110)-(1×2) at 300 K with monolayer coverage. (ii) Parallel polyethylene chains (bright lines) formed in the Au(110)-(1×3) reconstruction grooves by heating at 440 K for 30 min. (iii) High-resolution STM image of Au atomic rows and polyethylene chain. (iv) DEB monomers deposited on Au(110)-(1×2) at 300 K. (v) Polymerized DEB chains located in the Au(110)-(1×3) missing-row channels by heating at 420 K for 10 hours. The C–C coupling takes place between the terminal carbon atom of one molecule and the penultimate carbon atom of a neighboring molecule. (vi) A section of DEB polymer chain overlapped with the molecular model. The newly formed C–C bonds are shown in red. (Adapted with permission from ref. [58]. Copyright 2011 by the American Association for the Advancement of Science.)

Dehydrogenative homocouplings of sp^3-hybridized carbon atoms have also been demonstrated to fabricate one-dimensional carbon nanostructures. For example, In't Veld[57] et al. found that deposition of tetra(mesityl)porphyrin onto the Cu(110) surface with subsequent annealing leaded to the linkages between precursors. Later, Zhong[58] et al. also reported the alkyl C–H activation and subsequent C–C coupling on the Au(110) surface, leading to the formation of linear molecular chains. Experimentally,

n-dotriacontane ($C_{32}H_{66}$) was selected as a precursor, after deposition on an Au(110)-(1×2) surface at 300 K and followed by anneal at 400 K, the transition of the surface reconstruction from (1×2) to (1×3) and the formation of polymerized molecular chains within the grooves (as shown in **Figure 12a**) simultaneously occurred. STM tip manipulation and temperature-programmed desorption (TPD) were performed for further proving the covalent bonding between molecules and the generation of H_2 in the process of polymerization respectively. The dehydrogenative polymerization process of 1,4-di(eicosyl)benzene (DEB) was investigated as well. Similar to $C_{32}H_{66}$, the polymerization took place at 420 K with the surface reconstruction (as shown in **Figure 12b**). It was worth noting that phenylene rings arranged in either *anti*- or *syn*-conformation along the chains, and additional bright spots remarkably appeared roughly in the middle between the two neighboring phenylene groups. These bright spots were assigned to be methyl branches after comparing the distances of the bright spots to the two adjacent phenylene groups. Therefore, it could be concluded that C–C coupling can occur not only between the terminal methyl groups but also between a terminal methyl group and a penultimate methylene group. To further study the real active sites of Au(110) and explore the mechanism of the selective dehydrogenation of small alkanes, the same group performed other experiments and demonstrated that Au(110)-(1×3) surface can provide more active sites for C–H bond breaking[59]. Additionally, a representative establishment of one-dimensional conjugated polymers composed of indenofluorene units was shown by Di Giovannantonio[60] et al.

5. Others

This section aims for a brief introduction of the reactions containing more than one type of activation, and also for the generation of about the chirality during on-surface reaction.

Sonogashira coupling was considered to be one of the important reactions as well in solution chemistry, and it was also reported to occur on the surface in 2010[61]. Recent a representative work should be mentioned that the synthesis of graphyne nanowires via Sonogashira coupling was achieved on Ag(111)[62]. The delicately designed molecule 1,1'-biphenyl-4-bromo-4'-ethynyl (BPBE) showed high selectivity for Sonogashira coupling under the condition of high surface temperature, low molecular coverage, and low molecular evaporation rate. Heck coupling has also been implemented on the surface[63]. Highly selective cross-coupling of 5,15-bis(4-bromophenyl)-10,20-diphenylporphyrin and 5,10,15,20-tetrakis(4-bromophenyl)porphyrin with 4-vinyl-1,1'-biphenyl was shown on the Au(111) surface with the Pd catalyst.

Pavliček[64] and coworkers successfully generated tri-, tetra-, hexa- and octaynes on bilayer NaCl islands on Cu(111). Voltage pulses were applied to cleave C–Br bonds. Eventually, a series of polyynes was synthesized. It resembles the Fritsch–Buttenberg–Wiechell rearrangement reaction, and is totally different with Sun's work (ref. [38]). One important geometry feature of the products is the phenyl groups are often tilted out of the surface plane by a small angle, which accounted for the brighter parts of the phenyl in the constant-height AFM images.

The chirality is another issue within on-surface chemistry. Mairena[65] et al. compared the self-assembled structures of 9,9'-bisheptahelicene with the same species obtained by on-surface synthesis via Ullmann coupling, and it indicated that a surface may induce stereoselectivity by topochemistry.

6. Conclusions and outlooks

As summarized above, C–X and C–H activation of sp-, sp^2-, and sp^3-hybridized carbon atoms are all successfully implemented for on-surface fabrication of one-dimensional nanostructures. Brief conclusions could be drawn below: Ullmann coupling can be carried out on several surfaces (e.g., Au(111), Cu(111) and Ag(111)) with different activation temperatures, and C–X bond cleavage occurs at RT on Cu(111) and Ag(111) and ~450K on Au(111). Glaser coupling is preferred on the Ag(111) surface, with the typical temperature of ~350K. It is obvious that the research for on-surface synthesis of one-dimensional carbon nanostructures is thriving, whereas the types of reactions are still quite limited. In future works, on-surface chemistry may tend to study cross-coupling reactions, resembling organic reactions occurring in solution. This will make on-surface synthesis

strategies more diverse and flexible, and allow the construction of more complicated low-dimensional nanostructures. However, there still remains an open issue — how to control the reaction pathways with respect to cross-coupling and homocoupling, respectively. On the other hand, despite the fact that most of recent studies focus on analyzing final products, elucidation of the mechanisms is still of utmost importance and will be the key for us to understand on-surface reactions more thoroughly. In summary, the identification and analysis of reaction intermediates should be enhanced together with diverse on-surface analysis methods, such as TPD and DFT calculations.

Acknowledgements

The authors acknowledge financial supports from the National Natural Science Foundation of China (21622307, 21790351), the Fundamental Research Funds for the Central Universities.

Keywords: dehalogenative and dehydrogenative homocoupling reactions • one-dimensional materials • carbon-based nanostructures • on-surface synthesis • atomic precision

[1] a) C. Joachim, M. A. Ratner, Proc. Natl Acad. Sci. USA. **2005**, 102, 8801–8808; b) S. Eisler, A. D. Slepkov, E. Elliott, T. Luu, R. McDonald, F. A. Hegmann, R. R. Tykwinski, J. Am. Chem. Soc. **2005**, 127, 2666–2676; c) L. R. Radovic, B. Bockrath, J. Am. Chem. Soc. **2005**, 127, 5917–5927.

[2] H. Shirakawa, E. J. Louis, A. G. Macdiarmid, C. K. Chiang, A. J. Heeger, J.C.S. Chem. Comm. **1977**, 16, 578–580.

[3] a) F. Diederich, Nature **1994**, 369, 199–207; b) W. A. Chalifoux, R. R. Tykwinski, Nat. Chem. **2010**, 2, 967–971; c) A. Sun, J. W. Lauher, N. S. Goroff, Science **2006**, 312, 1030–1034; d) G. Li, Y. Li, H. Liu, Y. Guo, Y. Li, D. Zhu, Chem. Commun. **2010**, 46, 3256–3258.

[4] E. H. Falcao, F. Wudl, Chem. Technol. Biotechnol. **2007**, 82, 524–531.

[5] L. Grill, M. Dyer, L. Lafferentz, M. Persson, M. V. Peters, S. Hecht, Nat. Nanotechnol. **2007**, 2, 687–691.

[6] a) P. A. Held, H. Fuchs, A. Studer, Chem. Eur. J. **2017**, 23, 1–20; b) Q. Fan, J. M. Gottfried, J. Zhu, Acc. Chem. Res. **2015**, 48, 2484–2494; c) G. Otero, G. Biddau, C. Sánchez-Sánchez, R. Caillard, M. F. López, C. Rogero, F. J. Palomares, N. Cabello, M. A. Basanta, J. Ortega, J. Méndez, A. M. Echavarren, R. Pérez, B. Gómez-Lor, J. A. Martín-Gago, Nature **2008**, 454, 865–868; d) J. R. Sanchez-Valencia, T. Dienel, O. Groning, I. Shorubalko, A. Mueller, M. Jansen, K. Amsharov, P. Ruffieux, R. Fasel, Nature **2014**, 512, 61–64.

[7] G. Binnig, H. Rohrer, Ch. Gerber, E. Weibel, Appl. Phys. Lett. **1982**, 40, 178–180.

[8] Q. Sun, L. Cai, H. Ma, C. Yuan, W. Xu, ACS Nano **2016**, 10, 7023–7030.

[9] M. Liu, S. Li, J. Zhou, Z. Zha, J. Pan, X. Li, J. Zhang, Z. Liu, Y. Li, X. Qiu. ACS Nano **2018**, 12, 12612–12618.

[10] a) C. Glaser, Ann. Chem. Pharm. **1870**, 154, 137–171; b) C. Glaser, Ber. dtsch. chem. Ges. **1869**, 2, 422–424.

[11] Y.-Q. Zhang, N. Kepčija, M. Kleinschrodt, K. Diller, S. Fischer, A. C. Papageorgiou, F. Allegretti, J. Björk, S. Klyatskaya, F. Klappenberger, M. Ruben, J. V. Barth, Nat. Commun. **2012**, 3, 1286.

[12] H.-Y. Gao, H. Wagner, D. Zhong, J.-H. Franke, A. Studer, H. Fuchs, Angew. Chem. Int. Ed. **2013**, 52, 4024–4028.

[13] J. Liu, Q. Chen, L. Xiao, J. Shang, X. Zhou, Y. Zhang, Y. Wang, X. Shao, J. Li, W. Chen, G. Q. Xu, H. Tang, D. Zhao, K. Wu, ACS Nano **2015**, 9, 6305–6314.

[14] J. Liu, Q. Chen, Q. He, Y. Zhang, X. Fu, Y. Wang, D. Zhao, W. Chen, G. Q. Xu, K. Wu, Phys. Chem. Chem. Phys. **2018**, 20, 11081–11088.

[15] a) H. Klaasen, L. Liu, X. Meng, P. A. Held, H.-Y. Gao, D. Barton, C. Mück-Lichtenfeld, J. Neugebauer, H. Fuchs, A. Studer, Chem. Eur. J. **2018**, 24, 15303–15308. b) T. Lin, L. Zhang, J. Björk, Z. Chen, M. Ruben, J. V. Barth, F. Klappenberger, Chem. Eur. J. **2017**, 23, 15588–15593.

[16] B. Cirera, Y.-Q. Zhang, J. Björk, S. Klyatskaya, Z. Chen, M. Ruben, J. V. Barth, F. Klappenberger, Nano Lett. **2014**, 14, 1891–1897.

[17] Q. Sun, L. Cai, S. Wang, R. Widmer, H. Ju, J. Zhu, L. Li, Y. He, P. Ruffieux, R. Fasel, W. Xu, J. Am. Chem. Soc. **2016**, 138, 1106–1109.

[18] F. Ullmann, G. M. Meyer, O. Loewenthal, O. Gilli, Justus Liebig's Annalen der Chemie **1904**, 332, 38–41.

[19] S.-W. Hla, L. Bartels, G. Meyer, K.-H. Rieder, Phys. Rev. Lett. **2000**, 85, 2777–3780.

[20] T. Lin, X. Shang, J. Adisoejoso, P. Liu, N. Lin, J. Am. Chem. Soc. **2013**, 135, 3576–3582.

[21] J. Adisoejoso, T. Lin, X. Shang, K. Shi, N. Lin, Chem. Eur. J. **2014**, 20, 4111–4116.

[22] F. Ample, L. Grill, C. Joachim, H. Yu, L. Lafferentz, S. Hecht, Science **2009**, 323, 1193–1197.

[23] C. Bombis, F. Ample, L. Lafferentz, H. Yu, S. Hecht, C. Joachim, L. Grill, Angew. Chem. Int. Ed. **2009**, 48, 9966–9970.

[24] A. Saywell, J. Schwarz, S. Hecht, L. Grill, Angew. Chem. Int. Ed. **2012**, 51, 5096–5100.

[25] J. A. Lipton-Duffin, O. Ivasenko, D. F. Perepichka, F. Rosei, Small **2009**, 5, 592-597.

[26] L. Lafferentz, V. Eberhardt, C. Dri, C. Africh, G. Comelli, F. Esch, S. Hecht, L. Grill, Nat. Chem. **2012**, 4, 215–220.

[27] M. Di Giovannantonio, M. El Garah, J. Lipton-Duffin, V. Meunier, L. Cardenas, Y. F. Revurat, A. Cossaro, A. Verdini, D. F. Perepichka, F. Rosei, G. Contini, ACS Nano **2013**, 7, 8190–8198.

[28] S. Zint, D. Ebeling, T. Schlöder, S. Ahles, D. Mollenhauer, H. A. Wegner, A. Schirmeisen, ACS Nano **2017**, 11, 4183–4190.

[29] X. Zhou, C. Wang, Y. Zhang, F. Cheng, Y. He, Q. Shen, J. Shang, X. Shao, W. Ji, W. Chen, G. Xu, K. Wu, Angew. Chem. Int. Ed. **2017**, 56, 12852–12856.

[30] M. Di Giovannantonio, M. Tomellini, J. Lipton-Duffin, G. Galeotti, M. Ebrahimi, A. Cossaro, A. Verdini, N. Kharche, V. Meunier, G. Vasseur, Y. Fagot-Revurat, D. F. Perepichka, F. Rosei, G. Contini, J. Am. Chem. Soc. **2016**, 138, 16696–16702.

[31] D. Barton, H.-Y. Gao, P. A. Held, A. Studer, H. Fuchs, N. L. Doltsinis, J. Neugebauer, Chem. Eur. J. **2017**, 23, 6190–6197.

[32] Q. Fan, C. Wang, Y. Han, J. Zhu, W. Hieringer, J. Kuttner, G Hilt, J. M. Gottfried, Angew. Chem. Int. Ed. **2013**, 52, 4668–4672.

[33] J. Dai, Q. Fan, T. Wang, J. Kuttner, G. Hilt, J. M. Gottfried, J. Zhu, Phys. Chem. Chem. Phys. **2016**, 18, 20627–20634.

[34] Q. Fan, T. Wang, J. Dai, J. Kuttner, G. Hilt, J. M. Gottfried, J. Zhu, ACS Nano **2017**, 11, 5070–5079.

[35] J. Liu, T. Dienel, J. Liu, O. Groening, J. Cai, X. Feng, K. Müllen, P. Ruffieux, R. Fasel, J. Phys. Chem. C **2016**, 120, 17588–17593.

[36] J. I. Urgel, H. Hayashi, M. Di Giovannantonio, C. A. Pignedoli, S. Mishra, O. Deniz, M. Yamashita, T. Dienel, P. Ruffieux, H. Yamada, R. Fasel, J. Am. Chem. Soc. **2017**, 139, 11658–11661.

[37] a) H. Zhang, J.-H. Franke, D. Zhong, Y. Li, A. Timmer, O. D. Arado, H. Mönig, H. Wang, L. Chi, Z. Wang, K. Müllen, H. Fuchs, Small **2014**, 10, 1361–1368; b) H. Zhang, H. Lin, K. Sun, L. Chen, Y. Zagranyarski, N. Aghdassi, S. Duhm, Q. Li, D. Zhong, Y. Li, K. Müllen, H. Fuchs, L. Chi, J. Am. Chem. Soc. **2015**, 137, 4022–4025; c) H. Zhang, L. Chi, Adv. Mater. **2016**, 28, 10492–10498.

[38] Q. Sun, B. V. Tran, L. Cai, H. Ma, X. Yu, C. Yuan, M. Stöhr, W. Xu, Angew. Chem. Int. Ed. **2017**, 56, 12165–12169.
[39] K. S. Novoselov, A. K. Geim, S. V. Morozov, D. Jiang, Y. Zhang, S. V. Dubonos, I. V. Grigorieva, A. A. Firsov, Science **2004**, 306, 666–669.
[40] J. Cai, P. Ruffieux, R. Jaafar, M. Bieri, T. Braun, S. Blankenburg, M. Muoth, A. P. Seitsonen, M. Saleh, X. Feng, K. Müllen R. Fasel, Nature **2010**, 466, 470–473.
[41] J. van der Lit, M. P. Boneschanscher, D. Vanmaekelbergh, M. Ijäs, A. Uppstu, M. Ervasti, A. Harju, P. Liljeroth, I. Swart, Nat. Commun. **2013**, 4, 2023.
[42] D. S. L. Abergel, V. Apalkov, J. Berashevich, K. Ziegler, T. Chakraborty, Adv. Phys. **2010**, 59, 261–482.
[43] Q. Sun, R. Zhang, J. Qiu, R. Liu, W. Xu, Adv. Mater. **2018**, 30, 1705630.
[44] P. Han, K. Akagi, F. F. Canova, H. Mutoh, S. Shiraki, K. Iwaya, P. S. Weiss, N. Asao, T. Hitosugi, ACS Nano **2014**, 8, 9181–9187.
[45] D. G. de Oteyza, A. García-Lekue, M. Vilas-Varela, N. Merino-Díez, E. Carbonell-Sanromà, M. Corso, G. Vasseur, C. Rogero, E. Guitián, J. I. Pascual, J. E. Ortega, Y. Wakayama, D. Peña, ACS Nano **2016**, 10, 9000–9008.
[46] F. Schulz, P. H. Jacobse, F. F. Canova, J. van der Lit, D. Z. Gao, A. van den Hoogenband, P. Han, R. J.M. K. Gebbink, M.-E. Moret, P. M. Joensuu, I. Swart, P. Liljeroth, J. Phys. Chem. C **2017**, 121, 2896–2904.
[47] P. Ruffieux, S. Wang, B. Yang, C. Sánchez-Sánchez, J. Liu, T. Dienel, L. Talirz, P. Shinde, C. A. Pignedoli, D. Passerone, T. Dumslaff, X. Feng, K. Müllen, R. Fasel, Nature **2016**, 531, 489–493.
[48] C. Moreno, M. Vilas-Varela, B. Kretz, A. Garcia-Lekue, M. V. Costache, M. Paradinas, M. Panighel, G. Ceballos, S. O. Valenzuela, D. Peña, A. Mugarza, Science **2018**, 360, 199–203.
[49] Q. Sun, C. Zhang, H. Kong, Q. Tan, W. Xu, Chem. Commun. **2014**, 50, 11825–11828.
[50] Z. Cai, L. She, L. Wu, D. Zhong, J. Phys. Chem. C **2016**, 120, 6619–6624.
[51] C.-X. Wang, Q. Jin, C.-H. Shu, X. Hua, Y.-T. Long, P.-N. Liu, Chem. Commun. **2017**, 53, 6347–6350.
[52] J. Hellerstedt, A. Cahlík, O. Stetsovych, M. Švec, T. K. Shimizu, P. Mutombo, J. Klívar, I. G. Stará, P. Jelínek, I. Starý, Angew. Chem. Int. Ed. **2019**, 58, 2266–2271.
[53] X. Zhang, N. Xue, C. Li, N. Li, H. Wang, N. Kocić, S. Beniwal, K. Palotás, R. Li, Q. Xue, S. Maier, S. Hou, Y. Wang, ACS Nano **2019**, 13, 1385–1393.
[54] Q. Sun, L. Cai, Y. Ding, H. Ma, C. Yuan, W. Xu, Phys. Chem. Chem. Phys. **2016**, 18, 2730–2735.
[55] L. Cai, X. Yu, M. Liu, Q. Sun, M. Bao, Z. Zha, J. Pan, H. Ma, H. Ju, S. Hu, L. Xu, J. Zou, C. Yuan, T. Jacob, J. Björk, J. Zhu, X. Qiu, W. Xu, ACS Nano **2018**, 12, 7959–7966.
[56] Q. Sun, X. Yu, M. Bao, M. Liu, J. Pan, Z. Zha, L. Cai, H. Ma, C. Yuan, X. Qiu, W. Xu, Angew. Chem. Int. Ed. **2018**, 57, 4035–4038.
[57] M. In't Veld, P. Iavicoli, S. Haq, D. B. Amabilino, R. Raval, Chem. Commun. **2008**, 1536–1538.
[58] D. Zhong, J.-H. Franke, S. K. Podiyanachari, T. Blömker, H. Zhang, G. Kehr, G. Erker, H. Fuchs, L. Chi, Science **2011**, 334, 213–216.
[59] K. Sun, A. Chen, M. Liu, H. Zhang, R. Duan, P. Ji, L. Li, Q. Li, C. Li, D. Zhong, K. Müllen, L. Chi, J. Am. Chem. Soc. **2018**, 140, 4820–4825.
[60] M. Di Giovannantonio, J. Urgel, U. Beser, A. V. Yakutovich, J. Wilhelm, C. A. Pignedoli, P. Ruffieux, A. Narita, K. Müllen, R. Fasel, J. Am. Chem. Soc. **2018**, 140, 3532–3536.
[61] V. K. Kanuru, G. Kyriakou, S. K. Beaumont, A. C. Papageorgiou, D. J. Watson, R. M. Lambert, J. Am. Chem. Soc. **2010**, 132, 8081–8086.
[62] T. Wang, J. Huang, H. Lv, Q. Fan, L. Feng, Z. Tao, H. Ju, X. Wu, S. L. Tait, J. Zhu, J. Am. Chem. Soc. **2018**, 140, 13421–13428.
[63] K.-J. Shi, C.-H. Shu, C.-X. Wang, X.-Y. Wu, H. Tian, P.-N. Liu, Org. Lett. **2017**, 19, 2801–2804.
[64] N. Pavliček, P. Gawel, D. R. Kohn, Z. Majzik, Y. Xiong, G. Meyer, H. L. Anderson, L. Gross, Nat. Chem. **2018**, 10, 853–858.
[65] A. Mairena, C. Wäckerlin, M. Wienke, K. Grenader, A. Terfort, K.-H. Ernst, J. Am. Chem. Soc. **2018**, 140, 15186–15189.

REVIEW

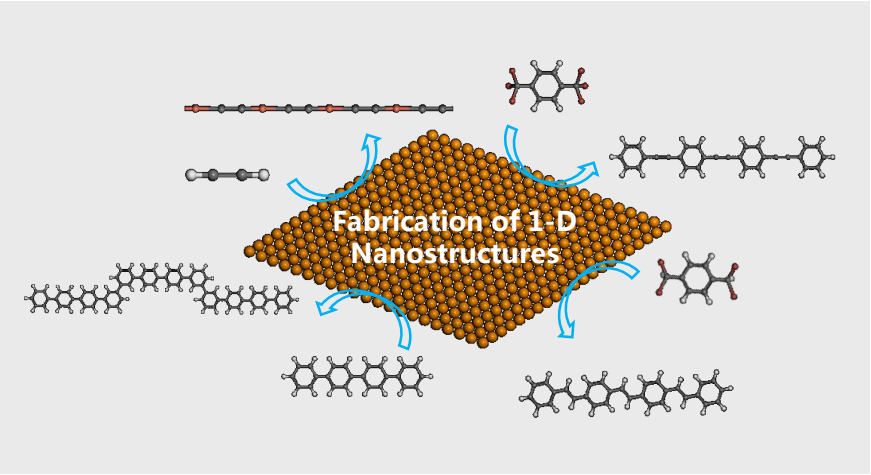

*F. Kang, W. Xu**

Page No. – Page No.

On-surface Synthesis of One-dimensional Carbon-based Nanostructures via C-X and C-H Activation Reactions

One-dimensional carbon-based nanostructures are of great interest to scientists for their great potential in many fields such as electronics and semiconductor physics. Metal surfaces can perform as templates as well as catalysts. Thus, on-surface chemistry is considered to be an efficient strategy for atomically precise fabrication of these nanostructures. In this article, we review the recent progresses of on-surface dehalogenative and dehydrogenative homocouplings of sp-, sp^2- and sp^3-carbon atoms, and various one-dimensional surface nanostructures are summarized.